X-Ray Study of Lattice Vibrations in Aluminum*

C. B. WALKER
Institute for the Study of Metals, University of Chicago, Chicago, Illinois
(Received April 27, 1956)

The diffuse scattering of monochromatic x-rays by a single crystal of aluminum at 300°K has been measured along seven lines in reciprocal space. Analysis of these data in terms of the Laval-James theory has yielded dispersion curves for elastic waves propagating along the three primary symmetry axes. By interpreting these dispersion curves in terms of the Born theory of lattice vibrations, values have been obtained for the nine force constants necessary to describe the general first-, second-, and third-neighbor interactions. These force constants have served as criteria in rejecting the simpler models of atomic interactions generally employed.

The secular equation containing these nine force constants has been solved for the eigenfrequencies of 2791 wave vectors by machine computation. These solutions served to establish an approximate frequency spectrum of the normal modes, in which the singularities caused by the critical points are explicitly included. From this spectrum the specific heat is calculated. A comparison with measured specific heats shows the need for the inclusion of anharmonic terms in the theoretical approach.

INTRODUCTION

THE early theory of lattice vibrations developed by Born and von Kármán[1] has been generalized and extended by Born and his colleagues.[2,3] In this general theory the equations of motion of the atoms in a lattice are developed in terms of harmonic tensor interatomic forces. Solution of the equations of motion in terms of plane wave normal coordinates leads to a secular equation relating the eigenfrequencies to the wave vectors of the traveling waves. An approximate spectrum of the frequencies of the normal modes can be obtained from the secular equation by several methods,[4–7] and from such a spectrum the lattice specific heat may be calculated in the usual way.

A primary problem in applying this general theory to specific lattices is that of evaluating the interatomic force constants for the particular lattice. If only elastic constant data are available, restrictive assumptions must be adopted concerning the nature of the interatomic forces in order that the number of nonzero force constants required by the theory not exceed the number of elastic constants. Thus the usual practice[5,8] in studying monatomic face-centered-cubic crystals has been to assume that the interatomic forces are central and limited to first and second neighbors, these requiring only two force constants. In comparison, the general theory requires three constants to describe first-neighbor interactions, two more to include second neighbors, and four more to include third neighbors. In the absence of experimental verification, the validity of these restrictions must be questioned.

X-ray diffuse scattering measurements offer a means of obtaining further data and thus a less restricted evaluation of these interatomic forces. Measurements of the intensity of the diffuse scattering of monochromatic x-rays by single crystals along particular lines in reciprocal space, after certain corrections, can yield directly the dispersion curves for the elastic waves propagating along the primary crystallographic axes. This method has been followed by several investigators[9–11] in studies of monatomic and diatomic crystals of cubic symmetry. One can extend this procedure to allow the determination of the general interatomic force constants by matching appropriate solutions of the secular equation to these measured dispersion curves. In this manner Curien[12] and Jacobsen[13] have determined the general force constants for first-, second-, and third-neighbor interactions in α-iron and copper, respectively. Joynson[14] has used a similar method to study force constants for the hexagonal lattice of zinc. In the following sections we shall review briefly the theory of this approach, paying particular attention to the necessary and often important corrections, and then apply it to a study of the lattice vibrations in aluminum.

DIFFUSE X-RAY SCATTERING

The theory of the diffuse scattering of x-rays arising from the thermal motion of the atoms of a lattice has been developed by Laval[15,16] and repeated in a somewhat different form by James.[17] Within the harmonic

* This work was supported by the Office of Ordnance Research, U. S. Army.

[1] M. Born and T. von Kármán, Physik. Z. **13**, 297 (1912); **14**, 15 (1913).
[2] M. Born and G. H. Begbie, Proc. Roy. Soc. (London) **A188**, 179 (1946).
[3] M. Born and K. Huang, *Dynamical Theory of Crystal Lattices* (Oxford University Press, London, 1954).
[4] W. V. Houston, Revs. Modern Phys. **20**, 161 (1948).
[5] R. B. Leighton, Revs. Modern Phys. **20**, 165 (1948).
[6] E. W. Montroll, J. Chem. Phys. **10**, 218 (1942); **11**, 481 (1943).
[7] M. Lax and J. L. Lebowitz, Phys. Rev. **96**, 594 (1954); H. B. Rosenstock, Phys. Rev. **97**, 290 (1955).
[8] C. W. Garland and G. Jura, J. Chem. Phys. **22**, 1108 and 1114 (1954).
[9] P. Olmer, Bull. soc. franç. minéral. **71**, 145 (1948); Acta Cryst. **1**, 57 (1948).
[10] H. Cole and B. E. Warren, J. Appl. Phys. **23**, 335 (1952).
[11] H. Cole, J. Appl. Phys. **24**, 482 (1953).
[12] H. Curien, Bull. soc. franç. minéral. **75**, 197 (1952); Acta Cryst. **5**, 392 (1952).
[13] E. H. Jacobsen, Phys. Rev. **97**, 654 (1955).
[14] R. E. Joynson, Phys. Rev. **94**, 851 (1954).
[15] J. Laval, Bull. soc. franç. minéral. **64**, 1 (1941).
[16] J. Laval, J. phys. radium **15**, 545 and 658 (1954).
[17] R. W. James, *The Optical Principles of the Diffraction of X-Rays* (G. Bell and Sons, London, 1948), Chap. 5.

oscillator approximation it is shown that the intensity of this scattering can be expressed as a series of terms, of which generally only the first three contribute appreciably. The first term, the first-order scattering, describes the intensity of the scattering in which a single phonon is involved. Similarly, the second- and third-order scattering terms describe the intensity of the scattering in which, respectively, two and three phonons are involved.

The first-order scattering in electron units per atom for a monatomic cubic crystal is given as

$$I_1(\mathbf{g})=\frac{f_0^2e^{-2M}}{m}\left|\frac{\mathbf{S}}{\lambda}\right|^2\sum_{j=1}^{3}\frac{E_{gj}\cos^2\alpha_{Sj}}{\nu_{gj}^2}, \quad (1)$$

where

$$E_{gj}=h\nu_{gj}\{[e^{h\nu_{gj}/kT}-1]^{-1}+\tfrac{1}{2}\}. \quad (2)$$

$I_1(\mathbf{g})$ is the intensity at a point in reciprocal space a vector distance $\mathbf{g}$ from the nearest reciprocal lattice point; f_0 and e^{-2M} are, respectively, the atomic scattering factor and the Debye temperature factor; m is the atomic mass, and $\mathbf{S}/\lambda$ is the diffraction vector, the difference between the wave vectors of the diffracted and incident x-rays. The sum over j is taken over the three independent elastic waves having the same wave vector $\mathbf{g}$ but different directions of vibration; ν_{gj} is the frequency of the jth such wave, α_{Sj} is the angle between its eigenvector and the diffraction vector $\mathbf{S}/\lambda$, and E_{gj} is its mean energy, which at room temperature may be significantly greater than the equipartition energy, kT.

This expression takes a much simpler form when the elastic wave vector $\mathbf{g}$ lies along one of the primary symmetry axes of the crystal, since such waves are characterized as being either pure longitudinal or pure transverse. Thus, the first-order scattering for $\mathbf{S}/\lambda$ (and hence $\mathbf{g}$) along a [100], [110], or [111] axis is

$$I_1(\mathbf{g})=\frac{f_0^2e^{-2M}}{m}\left|\frac{\mathbf{S}}{\lambda}\right|^2\frac{E_{gl}}{\nu_{gl}^2}, \quad (3)$$

and from this scattering one can determine directly the dispersion curves for these longitudinal waves. In a similar manner, dispersion curves for the transverse waves propagating along these directions can be determined from the first-order scattering along other particular lines in reciprocal space parallel to these axes, taken together with a knowledge of the dispersion of the corresponding longitudinal waves.

The above discussion describes the basis of the x-ray approach to the study of lattice vibrations. For a monatomic face-centered-cubic lattice, knowledge of the first-order scattering along seven particular lines in reciprocal space is sufficient to determine directly the dispersion curves for the longitudinal and transverse waves propagating along the three primary symmetry axes. Then by matching appropriate solutions of the secular equation to these experimental curves, one can evaluate the various interatomic force constants.

The scattering measured experimentally contains not only this first-order scattering but also the second- and third-order scattering and the incoherent Compton scattering. These other contributions must be either calculated or measured separately. It is in the evaluation of these correction terms, whose sum may often exceed the first-order scattering, that one finds a major source of error of this method.

The second-order scattering arises from processes in which pairs of phonons are involved. The intensity of this scattering at a point X in reciprocal space contains contributions from all pairs of elastic waves whose wave vectors, when added, extend from any reciprocal lattice point Q to the point X. Quantitatively

$$I_2(X)=\frac{f_0^2e^{-2M}}{2m^2}v\left|\frac{\mathbf{S}}{\lambda}\right|^4 \times\sum_Q\int\left\{\sum_{i,j=1}^{3}\sum\frac{E_iE_j}{\nu_i^2\nu_j^2}\cos^2\alpha_{Si}\cos^2\alpha_{Sj}\right\}dV_{QX}, \quad (4)$$

where v is the volume of the primitive unit cell. The indexes i and j refer to the three modes of vibration of the two waves whose wave vectors extend respectively from Q to dV_{QX} and from dV_{QX} to X. The integral extends over the volume V_{QX} common to first Brillouin zones centered on Q and X.

A rigorous calculation of this scattering cannot be made, since it requires in advance a complete knowledge of the eigenfrequencies and eigenvectors of all the elastic waves. One must depend on approximate calculations based on plausible yet simple assumptions as to the nature of the various waves. Olmer[9] developed a first approximation in which the crystal is assumed to be an ideal isotropic continuum, wherein all elastic waves have the same mean velocity. It may be expected that the assumption of isotropy will not cause a large error in these calculations. However, the neglect of dispersion and the characterization of both longitudinal and transverse waves by the same average velocity seem physically unrealistic and are capable of causing large errors. Thus a new calculation of this scattering was carried out in which the basic assumptions included dispersion according to a simple model and allowed differentiation of the longitudinal and transverse modes. Details of the calculation are given in the appendix. The intensity of the second-order scattering calculated in this way is significantly greater than that calculated from Olmer's approximation, particularly in the regions of reciprocal space where the first-order scattering is a minimum. The ratio of the second-order scattering to the first-order scattering, a maximum in such regions, is as much as 60% in the case of aluminum.

The third-order scattering, arising from processes involving three phonons, is much smaller in intensity. Little error is caused in this case by neglecting dispersion and associating an average velocity with all

elastic waves. Details of this calculation are contained in the article by Olmer.[9] In the present study, the ratio of the third-order scattering to the first-order scattering has a maximum value of approximately 6%.

The incoherent Compton scattering may form a large fraction of the total measured scattering, as was the case in the present study. The usual procedure in evaluating the intensity of this scattering has been to employ values calculated theoretically, such as those tabulated in Compton and Allison,[18] but Laval[19] has shown that these can be seriously in error. A reliable knowledge of this intensity can thus be obtained only from experimental measurements. The values of this intensity employed in the present study were determined experimentally; the procedure employed and the results obtained are discussed in a separate paper.[20] We will note here only the fact that the measured intensity of the Compton scattering was considerably lower than the theoretical values, in agreement with the results of Laval.

SECULAR EQUATION

In order to describe the general interactions between an origin atom and its first, second, and third neighbors in a monatomic face-centered-cubic lattice, a total of nine force constants are required. The secular equation for this lattice can be written in determinantal form as

$$|D(\mathbf{g})-\omega^2 I|=0. \tag{5}$$

The elements of $D(\mathbf{g})$ are[21]

$$D_{ii}(\mathbf{g})=\frac{4}{m}\left\{\begin{aligned}&\alpha_1[2-C_i(C_j+C_k)]+\beta_1(1-C_jC_k)\\&+\alpha_2S_i^2+\beta_2(S_j^2+S_k^2)+2\alpha_3(1-C_{2i}C_jC_k)\\&+2\beta_3[2-C_i(C_{2j}C_k+C_jC_{2k})]\end{aligned}\right\},$$

$$D_{ij}(\mathbf{g})=\frac{4}{m}\{S_iS_j(\gamma_1+2\gamma_3C_{2k})+2\delta_3C_k(S_{2i}S_j+S_iS_{2j})\},$$

$$S_i=\sin\pi g_i,\qquad C_i=\cos\pi g_i,$$

$$S_{2i}=\sin2\pi g_i,\quad C_{2i}=\cos2\pi g_i.$$

The quantity ω is the angular frequency of the elastic wave of wave vector $\mathbf{g}=g_1\mathbf{b}_1+g_2\mathbf{b}_2+g_3\mathbf{b}_3$, where $\mathbf{b}_i$ is the ith reciprocal lattice vector; $|\mathbf{b}_i|=a^{-1}$, where a is the real lattice constant. I is the unit matrix. The subscripts on the force constants, denoted by Greek letters, indicate the shell of neighboring atoms involved. These force constants are the second derivatives in a Taylor's series expansion of the total potential energy of the lattice. The particular meaning of each can be inferred from the more detailed notation given in Table I. In the particular case of central forces, $\alpha_1=\gamma_1$, $\beta_1=\beta_2=0$, and $\alpha_3=2\delta_3=4\beta_3=4\gamma_3$.

In the limit of long wavelengths, a comparison of the secular equation with elasticity theory yields the following relations:

$$\begin{aligned}aC_{11}&=4\alpha_1+4\alpha_2+16\alpha_3+8\beta_3,\\aC_{44}&=2\alpha_1+2\beta_1+4\beta_2+4\alpha_3+20\beta_3,\\a(C_{12}+C_{44})&=4\gamma_1+8\gamma_3+32\delta_3.\end{aligned} \tag{6}$$

EXPERIMENTAL PROCEDURE AND RESULTS

Aluminum single crystals were grown from a melt of aluminum of 99.99% purity by the usual Bridgman technique. Flat specimens were cut from these crystals, generally with faces parallel to (100) planes. These faces were prepared by mechanical polishing, etching in an aqueous cupric chloride solution, and electropolishing in a solution of one part HNO_3 to two parts of alcohol. Each crystal was examined both by the standard Laue method and by the special technique developed by Schulz.[22] The crystals accepted showed an angular spread of domains of less than ten minutes of arc.

Diffuse scattering measurements were made along seven lines in reciprocal space at room temperature, approximately 300°K, using CuKα radiation from a G.E. CA-7 tube powered by a full-wave rectified source at 50 kv and 16 ma. The radiation was monochromated by a toroidally bent LiF crystal so oriented as to focus the diffracted beam at the face of the specimen. Higher frequency harmonics passed by the monochromator were eliminated from the recorded scattered radiation with a balanced nickel-aluminum filter placed before the Geiger counter detector. Horizontal and vertical divergences of the primary beam were $\pm1°$. The single crystal specimen was mounted in a vacuum chamber, thus eliminating air scattering and minimizing the growth of the oxide film on the crystal. The face of the crystal was so oriented as to maintain equal angles with the incident and scattered beams, thus keeping the absorption correction angularly independent. The average counting time at any point in reciprocal space was approximately one hour for the nickel filter readings and $1\frac{1}{2}$ hours for the aluminum filter readings. The measured intensities were normalized to absolute units by the standard technique of comparison with the high angle scattering from amorphous substances. Paraffin, Lucite, and fused silica were used as amorphous materials, the interference function of the last named being found from a separate experiment with MoKα radiation. The three normalizations were internally consistent to better than 1% on using an experimentally measured value for the absorption coefficient of carbon.[23]

[18] A. H. Compton and S. K. Allison, *X-Rays in Theory and Experiment* (D. Van Nostrand Company, Inc., New York, 1935), second edition, p. 780.

[19] J. Laval, Compt. rend. **215**, 278 (1942).

[20] C. B. Walker, Phys. Rev. **103**, 558 (1956) following paper.

[21] These are equivalent to the elements given by Jacobsen (reference 13) after correction of typographical errors.

[22] L. G. Schulz, J. Metals **6**, 1082 (1954).

[23] The value measured, $\mu_m=4.23$ cm^2/g, agrees reasonably well with the value of 4.15 cm^2/g reported recently by D. R. Chipman, J. Appl. Phys. **26**, 1387 (1955).

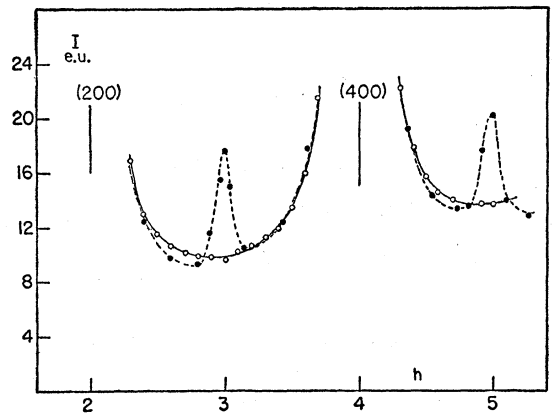

FIG. 1. Measured intensities along the [100] axis. The dotted curve joining the solid circles gives the results of Olmer, and the solid curve joining the open circles gives the present results. The abscissa is measured in units of the reciprocal cell edge, $|\mathbf{b}|$.

In the interpretation of the measurements, values for the atomic scattering factor were taken from the calculations of James and Brindley,[24] with a Honl factor of +0.18, as checked by the measurements of Brindley[25] and Brindley and Ridley.[26] The Debye temperature factor was based on an x-ray Θ_D of 402°K, checked by measurements on a low-temperature spectrometer; this value is 2% lower than that derived from the results of James, Brindley, and Wood.[27] Values for the elastic constants were taken as the mean of the values reported by Sutton,[28] Lazarus,[29] and Long and Smith.[30]

The measured intensities along the [100] axis in reciprocal space are compared in Fig. 1 with the corresponding data obtained by Olmer.[9] The peaks found by Olmer at the (300) and (500) positions are not found in the present measurements. It is believed that these peaks were caused by Bragg reflection of a $\lambda/2$ component in the primary beam and are not to be associated with the diffuse scattering.[31]

The first-order scattering along this axis was analyzed with Eq. (3) to give the experimental values for the dispersion of the [100] longitudinal waves plotted in Fig. 2. These values taken together with the measurements along the line from the (400) to the (420) reciprocal lattice points gave the values for the dispersion of the [100] transverse waves also plotted in Fig. 2. Similarly, measurements along lines from (222) to (333) and from (222) to (311) gave the values for the dispersion, respectively, of [111] longitudinal and transverse waves plotted in Fig. 3. Values for the dispersion of the [110] waves plotted in Fig. 4 were obtained from measurements along the lines from (220) to (29/8, 29/8, 0) (longitudinal), from (400) to (19/4, 19/4, 0) (transverse No. 1, $\mathbf{e}\|[001]$), and from (13/4, 11/4, 0) to (19/4, 5/4, 0) (transverse No. 2, $\mathbf{e}\|[1\bar{1}0]$).

An internal check on the validity of these data was made by comparing the limiting long-wavelength velocities extrapolated from these measurements with the velocities calculated from the elastic constants. Agreement within several percent was obtained for all except the [111] longitudinal waves, which gave an extrapolated velocity that was low by 7%. In view of the length of the extrapolation involved, this agreement is quite satisfactory.

These measured dispersion curves must be compared with the results of the x-ray investigations of Olmer[9] and Robert[32] and the neutron investigation of Brockhouse and Stewart.[33] After elimination of the effects of the false peaks, the values of ν *vs* g found by Olmer for the [100] longitudinal waves are somewhat greater than the present results, but the difference is within the combined errors of the original intensity measurements. Olmer's values for the [100] transverse waves are generally smaller than the present results, the greatest difference being about 15%. This difference is found to be due primarily to the different calculations of the second-order scattering correction, which have been

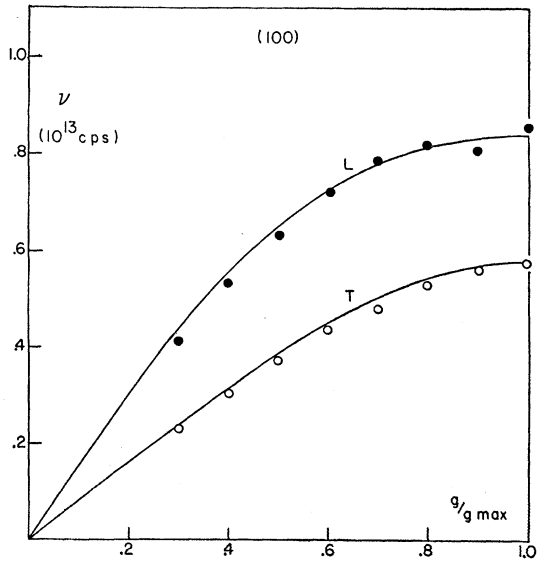

FIG. 2. Dispersion curves for elastic waves propagating along the [100] axis in aluminum. The measured data for the longitudinal and transverse waves are shown, respectively, by the solid and open circles. The smooth curves represent the fitted solutions of the secular equation.

[24] R. W. James and G. W. Brindley, Phil. Mag. **12**, 81 (1931).
[25] G. W. Brindley, Phil. Mag. **21**, 778 (1936).
[26] G. W. Brindley and P. Ridley, Proc. Phys. Soc. (London) **50**, 96 (1938).
[27] James, Brindley, and Wood, Proc. Roy. Soc. (London) **A125**, 401 (1925).
[28] P. M. Sutton, Phys. Rev. **91**, 816 (1953).
[29] D. Lazarus, Phys. Rev. **76**, 545 (1949).
[30] T. R. Long and C. S. Smith, Office of Naval Research Technical Report, July, 1953 (unpublished).
[31] Professor Olmer, in a personal communication, has agreed that this is the probable explanation of these peaks, for such a $\lambda/2$ component could have arisen from the faulty voltage regulation prevalent in Paris during the war.
[32] H. Robert, Bull. soc. franç. minéral **78**, 535 (1955).
[33] B. N. Brockhouse and A. T. Stewart, Phys. Rev. **100**, 756 (1955).

discussed in a previous section. Robert has recently reported on measurements of the dispersion of [111] longitudinal elastic waves. His results are completely different from the present values, showing for example a maximum frequency in this direction of approximately 0.50×10^{13} cps as compared with the value of 0.94×10^{13} cps found here. This disagreement can be traced to differences in the original intensity measurements, Robert's measurements being as much as 50% greater than the intensities measured in this study. We must conclude that there has been an error in the original measurements of Robert, since the present measurements were checked by separate measurements made on a second crystal with faces cut parallel to (111) planes, and there was agreement to within a few percent. Furthermore, a second check is offered by the measurements of Brockhouse and Stewart; their values for the dispersion of a very-short-wavelength [111] transverse wave and for a short-wavelength longitudinal wave whose wave vector is near the [111] axis agree within a few percent with the present results.

Solutions of the secular equation for waves propagating along the symmetry axes were then matched to these experimental points so as to give the best over-all fit and at the same time agree with the limiting ν *vs* g relations determined from the elastic constants. The smooth curves of Figs. 2, 3, and 4 represent these fitted solutions. The rather large scatter found in the experimental points for the short-wavelength longitudinal [111] and [110] waves clearly illustrates the magnification of errors that can arise during the subtraction of the correction terms. The largest deviations

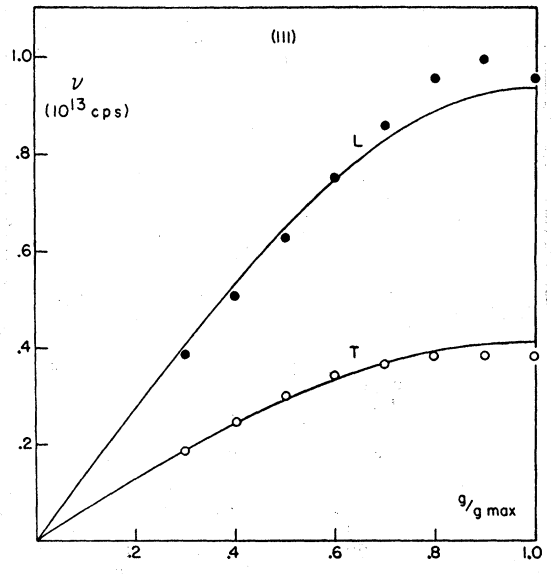

FIG. 3. Dispersion curves for elastic waves propagating along the [111] axis in aluminum. The measured data for the longitudinal and transverse waves are shown respectively by the solid and open circles. The smooth curves represent the fitted solutions of the secular equation.

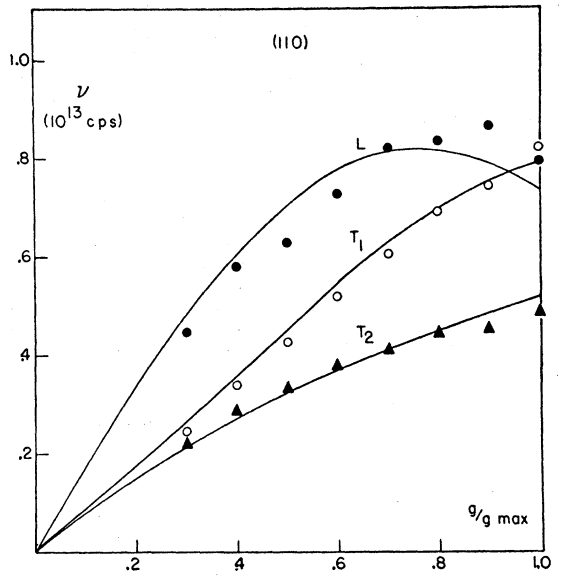

FIG. 4. Dispersion curves for elastic waves propagating along the [110] axis in aluminum. The measured data for the longitudinal wave are shown by the solid circles, the data for the transverse wave T_1 whose eigenvector is parallel to the [001] axis are given by the open circles, and the data for the transverse wave T_2 whose eigenvector is parallel to the $[1\bar{1}0]$ axis are given by the solid triangles. The smooth curves represent the fitted solutions of the secular equation.

in these cases could be due respectively to errors of $2\frac{1}{2}\%$ and 4% in the original intensity measurements.

The interatomic force constants obtained from these fitted solutions of the secular equation are listed in Table I under the heading A. The model of the interatomic forces employed here has required only that interactions beyond third neighbors be negligible. Also included in the table are the force constants for three more restricted models as evaluated from the x-ray and elastic constant data. The physical restrictions made for each model are listed in the caption.

An analysis of the errors has been carried out in order to evaluate the accuracy of the values determined for the nine force constants of the most general model. The quantities actually obtained from the fitted dispersion curves are the values for nine linear independent equations involving the various force constants. The standard deviations for these values have been found from a calculation based on the scatter of the experimental data combined with an estimate of the errors in the correction terms. The propagation of errors as these simultaneous equations are solved for the force constants then determines the accuracy with which any one constant is known. The results of the calculations are as follows: The relative error in the two primary-first neighbor force constants, α_1 and γ_1, is approximately 15%. The relative error in the primary second neighbor constant, α_2, is approximately 75%. The relative error for the other six constants, all of small magnitude, exceeds 100%.

TABLE I. Interatomic force constants[a] (in 10^3 dynes/cm) for aluminum. Model A neglects interactions beyond third neighbors. Model B considers only first- and second-neighbor forces, requiring the latter to be central. Model C allows only first-neighbor forces. Model D, the usual model, allows only central first- and second-neighbor forces.

	A	B	C	D
$\alpha_1=D(101)_{11}$	8.45	7.83	11.02	5.73
$\beta_1=D(101)_{22}$	−0.93	−2.10	−5.30	...
$\gamma_1=D(101)_{13}$	10.67	9.32	9.32	5.73
$\alpha_2=D(200)_{11}$	2.14	3.20	...	1.69
$\beta_2=D(200)_{22}$	0.40	...	...	...
$\alpha_3=D(211)_{11}$	0.27	...	...	...
$\beta_3=D(211)_{22}$	−0.31	...	...	...
$\gamma_3=D(211)_{23}$	0.10	...	...	...
$\delta_3=D(211)_{12}$	−0.19	...	...	...

[a] In the notation employed, $D(hkl)_{ij}$ may be considered as the force in the direction i on the origin atom due to a unit displacement in direction j of the atom at $\mathbf{r}=\frac{1}{2}h\mathbf{a}_1+\frac{1}{2}k\mathbf{a}_2+\frac{1}{2}l\mathbf{a}_3$.

The errors cited here refer to the accuracy with which any one constant is known, independent of all the others. Various linear combinations of the force constants are known to a much greater accuracy. For example, the elastic constant relations, Eq. (6), are known to approximately 1%, and certain other linear combinations obtained from the data for transverse waves are known to about 4%. Thus a frequency spectrum calculated from these force constants can be expected to be reasonably accurate, particularly at the lower frequencies.

The values for these nine force constants, despite their rather large errors, can still serve as effective criteria in an examination of the validity of the more restricted models of atomic interactions in aluminum. The Leighton two-constant model is not a valid approximation in this case, since its first-neighbor force constants are much too small. The three-constant model, model C, is also disallowed, for there are severe discrepancies in several constants. The simplest model based on the Born theory that can describe the interactions in aluminum within the limits established by the present experiment is a four-constant model based on general first-neighbor forces and a central second-neighbor force.

FREQUENCY SPECTRUM, CRITICAL POINTS, AND SPECIFIC HEAT

The solutions of the secular equation employing the experimental values of the nine force constants listed in Table I were calculated and tabulated by the electronic computer AVIDAC at the Argonne National Laboratory for the 2791 wave vectors distributed on a cubic net[34] through the volume element of the first Brillouin zone irreducible under symmetry operations. These eigenfrequencies were used to determine histograms of the frequency spectra of the normal modes and to locate and characterize the several critical points occurring in the various branches.

[34] The net interval is $(1/30)|\mathbf{b}|$.

The histograms of the frequency spectra of the different branches are given in Fig. 5. The "longitudinal," "high transverse," and "low transverse" branches have been defined as containing respectively the high-, middle-, and low-frequency solutions for a given wave vector.[35] This definition was adopted so that in a given branch the frequency would be a continuous function of the wave vector. The histogram of the total frequency spectrum is given in Fig. 6.

Van Hove[36] has shown that as a result of the periodicity of a crystal, its wave-vector space will show certain critical points which cause singularities in the elastic frequency spectrum. These critical points are the points in wave-vector space at which the gradient of the frequency of a given branch vanishes. The topological nature of the surfaces of constant frequency near a critical point determines the shape of the frequency spectrum near this critical frequency. Van Hove discussed quantitatively the singularities arising from analytic critical points and derived from topological arguments a minimum number of the various types of critical points which must occur for each branch. Phillips[37] has derived quantitative descriptions

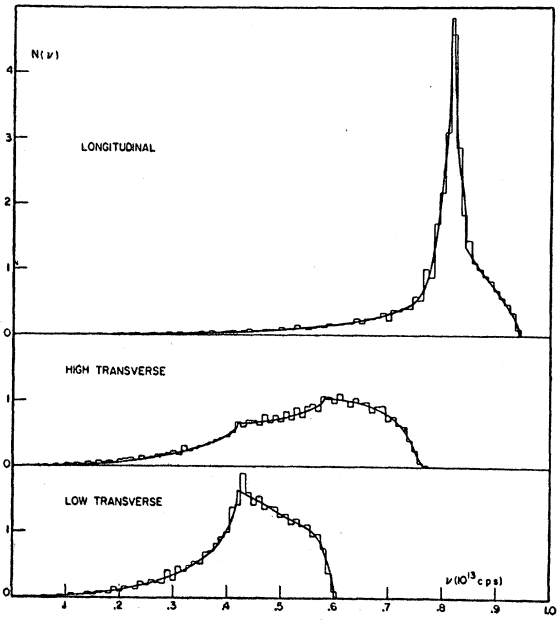

FIG. 5. Vibrational frequency spectra for the three branches of aluminum. The histograms are obtained from computed eigenfrequencies for 2791 wave vectors. The smooth curves are obtained from the histograms together with the inclusion of the singularities caused by the various critical points.

[35] The eigenvectors for the low-frequency solutions in a branch as so defined are described reasonably well by its title, i.e., longitudinal or transverse, but this is not necessarily true for the high frequencies. For example, the solution assigned to the "longitudinal" branch for the wave of minimum wavelength propagating along a [110] axis actually corresponds to a pure transverse wave; this results from the crossing of two dispersion curves as shown in Fig. 4.

[36] L. Van Hove, Phys. Rev. 89, 1189 (1953).

[37] J. C. Phillips (to be published).

of the singularities arising from various types of nonanalytic critical points.[38] Phillips also has further extended Van Hove's treatment, deriving from group theoretical and topological considerations a series of relations which define a minimal set of critical points, both analytic and nonanalytic, which must occur in a given branch. In the examples to which these relations have been applied, this minimal set has proved identical to the actual set of critical points present.

In order to obtain the best representation of the frequency spectrum, one must thus locate and characterize all of the critical points for the different branches. Some are easily located from the symmetry of the first Brillouin zone, as, for example, the centers of (100) and (111) faces for face-centered-cubic crystals. Until the development of Phillips' relations, the location of all the other points could be quite difficult.[39] Given the sets of frequencies tabulated by the computer, the simplest procedure for locating and characterizing these points in the present case was to plot contours of constant frequency on several planes through the Brillouin zone.

All the critical points for aluminum were found to be on either (100) or (110) planes. The constant-frequency contours for these planes are given in Fig. 7. The critical points found included the various analytic types, such as the maxima M and the saddle points S_1 and S_2, and also several of nonanalytic behavior, those denoted as N_1, N_2, M_N, S_{2N}, and D.[40] Using the known shape of the frequency spectrum near these critical frequencies, the best approximation to the frequency spectrum of aluminum at 300°K was determined. This is shown by the continuous curves of Figs. 5 and 6. By comparison, a Debye spectrum giving the measured specific heat at this temperature has $\Theta_D=382$°K; its cut-off frequency is then 0.796×10^{13} cps.

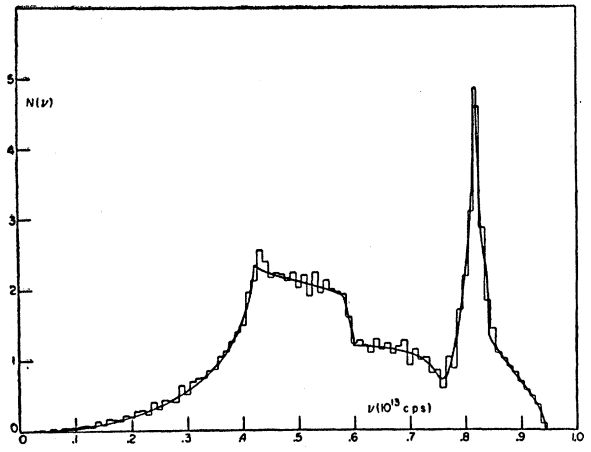

FIG. 6. Total vibrational frequency spectrum for aluminum at 300°K. The histogram is obtained from 8373 calculated eigenfrequencies. The smooth curve is obtained from the histogram after inclusion of the singularities arising from the critical points of the various branches.

Using the approximate spectrum of Fig. 6, the lattice specific heat at constant volume was calculated from the usual relation,

$$C_V=3R\int_0^{\nu_m}\frac{x^2e^x}{(e^x-1)^2}N(\nu)d\nu, \tag{7}$$

where

$$x=h\nu/kT, \quad \int_0^{\nu_m}N(\nu)d\nu=1.$$

The results are shown as the solid circles of Fig. 8. The smooth curve is drawn through the experimental values of Giauque and Meads,[41] corrected for electronic contributions as measured by Howling, Mendoza, and Zimmerman.[42] Although there is reasonable agreement at the higher temperatures, the calculated values are significantly higher at the lower temperatures, the maximum deviation being about 24%. This error is about twice that which could have been caused by errors in the experimental force constants, since at these temperatures only the well-determined low-frequency part of the spectrum is effective.

There is a primary restriction that appears in all phases of the theory involved in this study, namely, that the atomic oscillations be harmonic. In order to estimate an order of magnitude of the effect of the inclusion of anharmonic terms, the following simple approach has been used. It is assumed that the anharmonic terms can be included in the Born theory by describing the atomic interactions as harmonic forces which vary with temperature. It is further assumed that all the force constants show the same relative dependence on temperature.[43] Within these assumptions, the effect of anharmonicity is only to cause the scale of the frequency distribution to be a function of temperature. On neglecting the small extra term which will appear in the expression for the specific heat, Eq. (7), this modification of the scale of the frequency spectrum simply causes the specific heats calculated at different temperatures from the harmonic theory to be associated with similarly modified temperatures. The modifying multiplicative factor is given by the square root of the mean measured variation of the elastic constants.[28]

The specific heats calculated by this method of including anharmonic terms are plotted as the open

[38] A critical point is described as nonanalytic if the surfaces of constant frequency around it cannot be described in terms of a Taylor's series expansion. Such behavior arises from the degeneracy of two or more branches at this point.

[39] See the article by Rosenstock, reference 7.

[40] These nonanalytic critical points, certain of which are termed "accidental," must be expected to occur for any real monatomic face-centered-cubic crystal.

[41] W. F. Giauque and P. F. Meads, J. Am. Chem. Soc. **63**, 1897 (1941).

[42] Howling, Mendoza, and Zimmerman, Proc. Roy. Soc. (London) **A229**, 86 (1955).

[43] The degree of validity of this assumption is indicated by the variations of up to 30% found in the relative change of the elastic constants of aluminum with temperature by Sutton (reference 28).

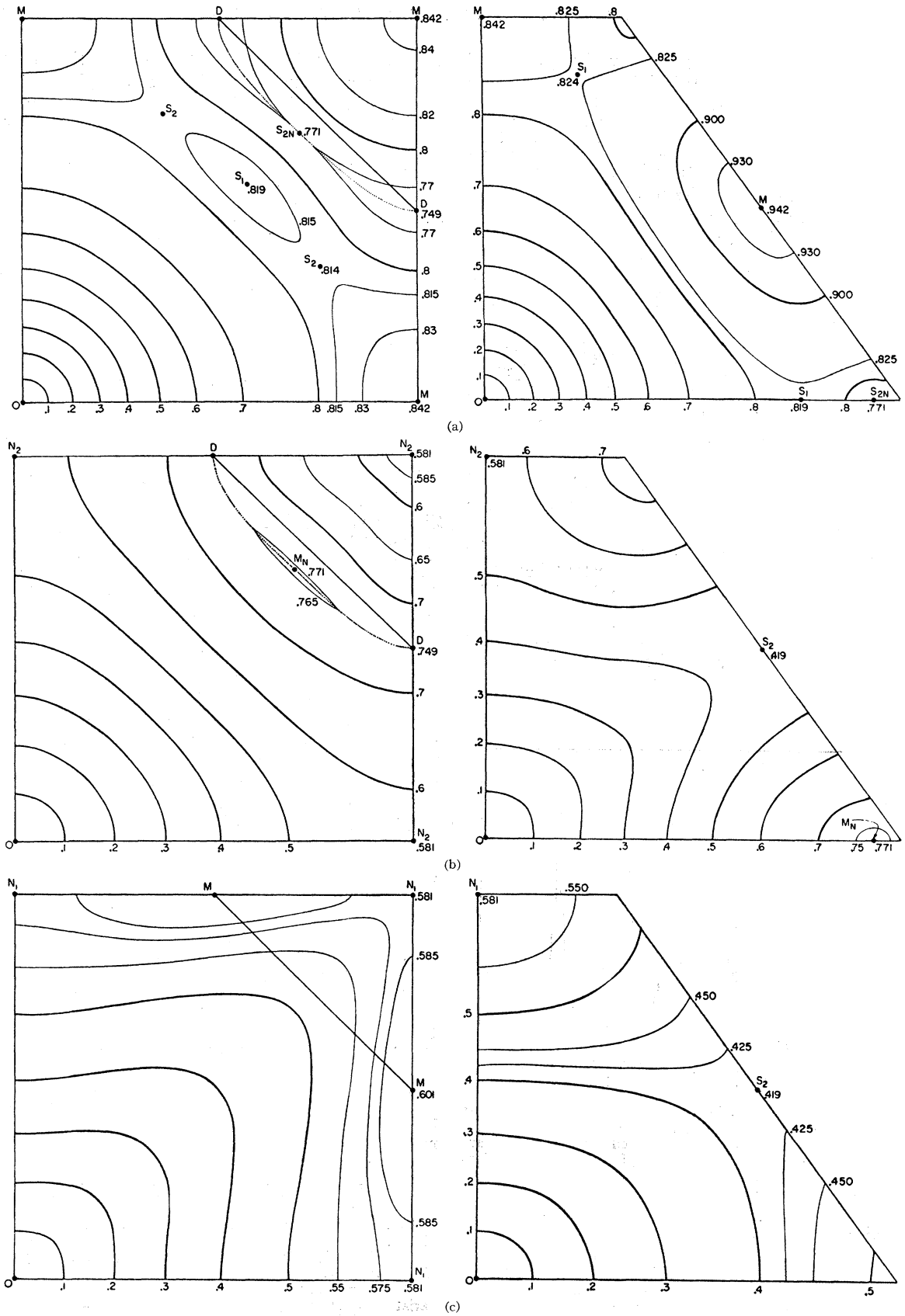

FIG. 7. Constant-frequency contours on (100) and (110) planes for the three branches of aluminum. The lettered solid circles denote the various critical points. (a) Longitudinal branch. The dotted line in the (100) plane extending between the points D and passing through the nonanalytic saddle point S_{2N} represents the locus of the points of degeneracy between this branch and the high transverse branch. (b) High transverse branch. (c) Low transverse branch.

circles of Fig. 8. Agreement with the experimental curve of the specific heat is quite good. The previous error of 24% is reduced here to only 9%, which is within the accuracy to be expected from errors in the force constants.

These calculated specific heats are replotted in terms of Debye temperatures in Fig. 9. The calculations which include the correction for anharmonicity, given as curve *B*, show quite good agreement with the experimental measurements.

DISCUSSION

The first objective of this investigation has been the determination of the force constants which describe the general interactions between first, second, and third neighbors in aluminum. The values for these nine constants are listed in Table I. An analysis of the propagation of errors has shown that, although several linear combinations of these constants are known to within a few percent, only three of the constants are known individually to within 100%; these are the primary first-neighbor constants α_1 and γ_1, known to 15%, and the primary second-neighbor constant α_2, known to 75%. These errors illustrate clearly the limitations of this x-ray method. The unavoidable errors in measurements and in the correction for Compton and second- and third-order scattering are magnified by the subtraction of the correction terms, and the accumulation of these errors leads to great uncertainty in the force constants that have small absolute values. Greater accuracy should be possible for studies of elements of higher atomic number, since the relative size of their corrections will be smaller, but error accumulation should still prevent an accurate knowledge of the small force constants.

The results of this analysis of the force constants have been used to examine the validity of some of the more restricted models of atomic interactions in aluminum. Both the usual two-constant model, involving central first- and second-neighbor forces, and a model based on only general first-neighbor forces failed to satisfy these experimental criteria. The simplest model based on the Born theory that will describe the interactions in aluminum within the experimental limits of errors is the four-constant model based on general first-neighbor forces and a central second-neighbor force. Considerably smaller rms deviations between the measured and calculated dispersion curves are obtained for the general, nine-constant model, but the possible errors in the measured values are such that the use of this model, while perhaps of value, is not required.

An approximate frequency spectrum of the normal modes has been calculated in which the singularities arising from the critical points have been explicitly included. The specific heat calculated from this spectrum shows good agreement with the measured values at room temperature, but is systematically greater

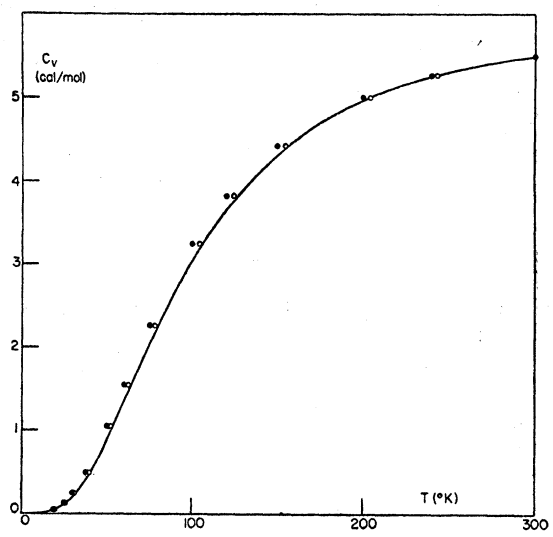

FIG. 8. Specific heat as a function of temperature. The solid line is drawn through the experimental values of Giauque and Meads, corrected for the electronic contribution. The solid circles represent values calculated directly from the spectrum of Fig. 6. The open circles represent similar calculations with an approximate inclusion of anharmonic terms.

than the measurements at the lower temperatures, the difference being too large to be due to errors in the force constants. A simple calculation has shown that the majority of this difference can easily be attributed to the omission of anharmonic terms in the theory. These terms have been neglected not only in the Born theory of lattice vibrations but also in the theory of x-ray scattering and in the development from Boltzmann statistics of the relation for the specific heat. The inclusion of anharmonicity considerably complicates these

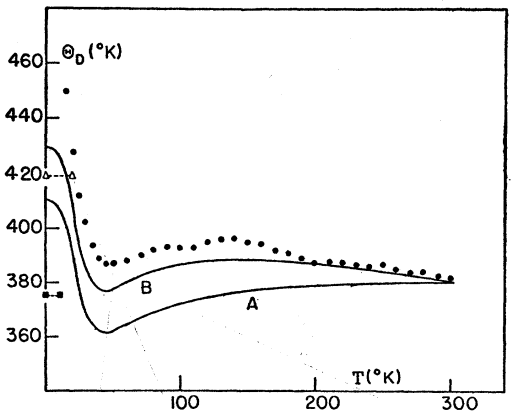

FIG. 9. Debye temperature as a function of temperature. The solid circles are obtained from the measurements of Giauque and Meads, corrected for the electronic contribution. The solid squares give the results measured by Howling, Mendoza, and Zimmerman and the open triangles give the values determined by Kok and Keesom [Physica 4, 835 (1937)]. Curve *A* is obtained from the directly calculated specific heats, and curve *B* is obtained from similar calculations which have included an approximation for anharmonic terms.

theories, and as yet this problem has not been satisfactorily resolved. It is in this direction that progress must be made if a better understanding of the interatomic interactions in crystals is to be achieved.

The author is particularly indebted to Dr. D. A. Flanders of the Argonne National Laboratory for the advice and discussions on computer techniques given on many occasions.

APPENDIX

On assuming equipartition of energy between all modes, the expression for the second-order thermal scattering, Eq. (4), takes the form

$$I_2(X)=\frac{f_0^2e^{-2M}}{2m^2}v(kT)^2\left|\frac{\mathbf{S}}{\lambda}\right|^4 \times\sum_Q\int\left\{\sum_{i,j=1}^{3}\sum\frac{\cos^2\alpha_{Si}}{\nu_i^2}\frac{\cos^2\alpha_{Sj}}{\nu_j^2}\right\}dV_{QX}. \quad (8)$$

The definition of the various quantities is given in the main text. We shall adopt the following assumptions:

(a) The actual first Brillouin zone can be described as a sphere of the same volume, whose radius is the maximum wave vector, g_m.

(b) The crystal is elastically isotropic. The waves of a given wave vector are thus pure longitudinal or pure transverse, and the transverse branches are degenerate.

(c) The dispersion of the waves of any branch is given by the simple linear chain relation,

$$\nu=V\frac{2g_m}{\pi}\sin\left(\frac{\pi}{2}\frac{g}{g_m}\right). \quad (9)$$

The long-wavelength velocity V for the different branches is obtained by averaging the appropriate velocities for long-wavelength waves propagating along the three primary symmetry axes.

We consider first the contribution to this intensity at the point X in reciprocal space from the normal modes for the particular pair of wave vectors required by the choice of the reciprocal lattice point Q and the volume element dV_{QX}. The eigenvectors for these modes and the unit vector along $\mathbf{S}/\lambda$ are described in terms of the coordinate system shown in Fig. 10. The intensity from this pair of wave vectors is averaged as the eigenvectors for the transverse waves take all orientations. Next one integrates over φ, the angular variable for which the magnitudes of g_1 and g_2 remain invariant. The cumbersome mathematical form of the results is considerably simplified by the following notation.

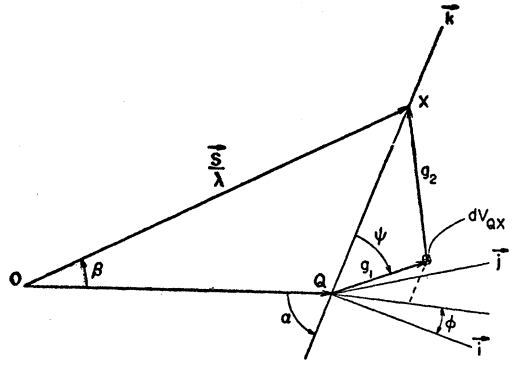

FIG. 10. Diagram for the calculation of the second-order scattering. The unit vector $\mathbf{i}$ is contained in the plane defined by the line segments OQ and QX.

Let

$$g_1/g_m=x, \quad |QX|/g_m=p$$

(where $|QX|$ denotes the length of the line segment from Q to X), so that

$$g_2/g_m=(x^2+p^2-2px\cos\psi)^{\frac{1}{2}}.$$

Let

$$H=\frac{x^2}{\sin^2(\frac{1}{2}\pi x)\sin^2[\frac{1}{2}\pi(x^2+p^2-2px\cos\psi)^{\frac{1}{2}}]},$$

$$A=\int Hdx, \quad B=\int\frac{x^2}{x^2+p^2-2px\cos\psi}Hdx,$$

$$C=\int\frac{2px\cos\psi}{x^2+p^2-2px\cos\psi}Hdx,$$

and let

$$F_0=\left[\frac{\pi^2}{4}\frac{k^2}{(1+\frac{2}{3}k)^2}\right]E_0=\left[\frac{\pi^2}{4}\frac{k^2}{(1+\frac{2}{3}k)^2}\right]\int A\sin\psi d\psi,$$

$$\gamma_1=\frac{1}{E_0}\int A\sin^3\psi d\psi, \quad \gamma_2=\frac{1}{E_0}\int B\sin^3\psi d\psi,$$

$$\gamma_3=\frac{1}{E_0}\int C\sin^3\psi d\psi, \quad \gamma_4=\frac{1}{E_0}\int B\sin^5\psi d\psi,$$

where

$$1+k=V_t^2/V_t^2.$$

Then

$$\frac{I_2(X)}{Z}=\sum_Q F_0\{R^2+RS\gamma_1+(RS+2V)\gamma_2 -V\gamma_3+(S^2+T-2V)\gamma_4\}, \quad (10)$$

where

$$Z=\frac{f_0^2e^{-2M}}{2m^2}\frac{v(kT)^2\pi^3}{V_m^4g_m}\left|\frac{\mathbf{S}}{\lambda}\right|^4,$$

$$R=[(1/k)+\sin^2(\alpha-\beta)], \quad T=\tfrac{1}{8}\sin^4(\alpha-\beta),$$

$$S=[1-\tfrac{3}{2}\sin^2(\alpha-\beta)], \quad V=\sin^2(\alpha-\beta)\cos^2(\alpha-\beta),$$

$$\frac{1}{V_m^2}=\frac{1}{3}\left(\frac{1}{V_l^2}+\frac{2}{V_t^2}\right).$$

The limits of the integrals, functions of the parameter p, are such that the integration extends over that half of the volume common to the Brillouin zones centered on Q and X for which $|\mathbf{g}_1| \leq |\mathbf{g}_2|$. The integrals in this expression have been evaluated numerically for various values of the parameter p and are tabulated in Table II. The total second-order scattering at any point X is found by summing the contributions associated with each of the reciprocal lattice points Q.

An important feature of this expression, Eq. (10), is that it allows the contribution to the scattering at X associated with the reciprocal lattice point Q, to depend on the angle between QX and $\mathbf{S}/\lambda$. The angular dependence is a function of the parameter p, ranging from no dependence at $p=0$ to a maximum dependence at $p=2$, where this intensity can vary by a factor of about 20 for aluminum. Such a directional dependence, not allowed in the calculation by Olmer, is easily understood; the intensity varies effectively as $(\bar{\nu})^{-4}$ and so must depend markedly on whether the majority of the contributing waves are transverse, with low frequencies, or longitudinal, with higher frequencies. When the total second-order scattering is formed by summing the contributions from all reciprocal lattice points, the net directional dependence is reduced but remains of the order of a factor of 2. The net result of this effect plus the inclusion of dispersion gives an intensity of the second order scattering which may be as much as three times the intensity calculated by Olmer. This difference is generally significant.

TABLE II. Data for calculation of second-order scattering from Eq. (10).

p	E_0	γ_1	γ_2	γ_3	γ_4
0	∞	0.666	0.666	0.000	0.533
0.2	2.220				
0.4	1.161	0.724	0.281	0.098	0.243
0.6	0.782				
0.8	0.550	0.715	0.196	0.218	0.156
1.0	0.307				
1.2	0.124	0.406	0.215	0.536	0.110
1.4	0.050				
1.6	0.021	0.165	0.131	0.434	0.030
1.8	0.005				
2.0	0.000	0.000	0.000	0.000	0.000

A similar calculation can be carried out for the scattering at very low temperatures. The only significant change is that the energy of a mode is taken as its zero-point energy, $\frac{1}{2}h\nu$, rather than kT. This calculation has been carried out and applied to aluminum, with the interesting and unforeseen result that even at absolute zero the second-order scattering is not negligible.